10

CARBON–CEMENT COMPOSITES

D. D. L. Chung

1 Introduction

Carbon–cement composites refer to cement–matrix composites that contain carbon (e.g. carbon fibers). Carbon in a discontinuous form is usually used, because this form can be added to the cement mix in the mixer (i.e. it can be used as an admixture). In contrast, carbon in a continuous form cannot be used as an admixture. Mixing is the most convenient way of incorporating any ingredient in a cement-based material. Not only is mixing inexpensive, it can be done in the field. Another disadvantage of using continuous carbon fibers is the high cost of continuous fibers compared to discontinuous fibers. Low cost is essential for a concrete to be practical. Although there are many forms of discontinuous carbon, short carbon fibers are the only form that has been shown to be useful for improving the properties of cement-based materials. Therefore, this chapter is focused on cement–matrix composites containing short carbon fibers.

Carbon fiber cement–matrix composites are structural materials that are gaining in importance quite rapidly due to the decrease in carbon fiber cost (Newman, 1987) and the increasing demand of superior structural and functional properties. These composites contain short carbon fibers, typically 5 mm in length. However, due to the weak bond between carbon fiber and the cement matrix, continuous fibers (Furukawa *et al*., 1987; Saito *et al*., 1989; Wen and Chung, 1999a) are much more effective than short fibers in reinforcing concrete. Surface treatment of carbon fiber (e.g. by heating (Sugama *et al*., 1989) or by using ozone (Fu *et al*., 1996, 1998a), silane (Xu and Chung, 1999a, 2000), SiO_2 particles (Yamada *et al*., 1991) or hot NaOH solution (Sugama *et al*., 1988)) is useful for improving the bond between fiber and matrix, thereby improving the properties of the composite. In the case of surface treatment by ozone or silane, the improved bond is due to the enhanced wettability by water. Admixtures such as latex (Fu *et al*., 1996; Larson *et al*., 1990), methylcellulose (Fu *et al*., 1996) and silica fume (Katz *et al*., 1995) also help the bond.

The effect of carbon fiber addition on the properties of concrete increases with fiber volume fraction (Park and Lee, 1993), unless the fiber volume fraction is so high that the air void content becomes excessively high (Chen *et al*., 1997). (The air void content increases with fiber content and air voids tend to have a negative effect on many properties, such as the compressive strength.) In addition, the workability of the mix decreases with fiber content (Park and Lee, 1993). Moreover, the cost increases with fiber content. Therefore, a rather low volume fraction of fibers is desirable. A fiber content as low as 0.2 vol% is effective (Chen and Chung, 1993a), although fiber contents exceeding 1 vol% are more common (Akihama *et al*., 1984; Brandt and Kucharska, 1996). The required fiber content increases

with the particle size of the aggregate, as the flexural strength decreases with increasing particle size (Kamakura *et al*., 1983).

Effective use of the carbon fibers in concrete requires dispersion of the fibers in the mix. The dispersion is enhanced by using silica fume (a fine particulate) as an admixture (Ohama and Amano, 1983; Ohama *et al*., 1985; Katz and Bentur, 1994; Chen *et al*., 1997). A typical silica fume content is 15% by weight of cement (Chen *et al*., 1997). The silica fume is typically used along with a small amount (0.4% by weight of cement) of methylcellulose for helping the dispersion of the fibers and the workability of the mix (Chen *et al*., 1997). Latex (typically 15–20% by weight of cement) is much less effective than silica fume for helping the fiber dispersion, but it enhances the workability, flexural strength, flexural toughness, impact resistance, frost resistance and acid resistance (Soroushian *et al*., 1991; Zayat and Bayasi, 1996; Chen *et al*., 1997). The ease of dispersion increases with decreasing fiber length (Ohama *et al*., 1985).

The improved structural properties rendered by carbon fiber addition pertain to the increased tensile and flexible strengths, the increased tensile ductility and flexural toughness, the enhanced impact resistance, the reduced drying shrinkage and the improved freeze-thaw durability (Kamakura *et al*., 1983; Ohama and Amano, 1983; Akihama *et al*., 1984; Ohama *et al*., 1985; Lal, 1990; Park and Lee, 1990; Soroushian, 1990; Park *et al*., 1991; Soroushian *et al*., 1992a,b; Park and Lee, 1993; Toutanji *et al*., 1993; Chen and Chung, 1993a; Katz and Bentur, 1994; Banthia *et al*., 1994a,b, 1998; Banthia and Sheng, 1996; Pigeon *et al*., 1996; Zayat and Bayasi, 1996; Chen *et al*., 1997). The tensile and flexural strengths decrease with increasing specimen size, such that the size effect becomes larger as the fiber length increases (Urano *et al*., 1996). The low drying shrinkage is valuable for large structures and for use in repair (Chen *et al*., 1995; Ali and Ambalavanan, 1998) and in joining bricks in a brick structure (Zhu and Chung, 1997; Zhu *et al*., 1997).

The functional properties rendered by carbon fiber addition pertain to the strain sensing ability (Chen and Chung, 1993b, 1995a, 1996a,b; Chung, 1995; Zhao *et al*., 1995; Fu and Chung, 1996, 1997a; Mao *et al*., 1996a,b; Fu *et al*., 1997, 1998a,b; Sun *et al*., 1998, 2000; Shi and Chung, 1999; Wen and Chung, 2000a, 2001a,b, 2002a,b) (for smart structures), the temperature sensing ability (Sun *et al*., 1998a,b; Wen and Chung, 1999b, 2000b–d), the damage sensing ability (Chen and Chung, 1993b, 1996b; Lee and Batson, 1996; Bontea *et al*., 2001; Wen and Chung, 20001f), the thermoelectric behavior (Chen and Chung, 1993b, 1996b; Sun *et al*., 1998a,b; Wen and Chung, 1999c, 2000b–d), the thermal insulation ability (Shinozaki, 1990; Fu and Chung, 1999; Xu and Chung, 1999b) (to save energy for buildings), the electrical conduction ability (Clemena, 1988; Banthia *et al*., 1992; Chen and Chung, 1993c, 1995b; Fu and Chung, 1995; Shui *et al*., 1995; Xie *et al*., 1996; Brousseau and Pye, 1997; Hou and Chung, 1997; Wang *et al*., 1998; Wen and Chung, 2001c–f) (to facilitate cathodic protection of embedded steel and to provide electrical grounding or connection), and the radio wave reflection/absorption ability (Shimizu *et al*., 1986; Fujiwara and Ujie, 1987; Fu and Chung, 1997b, 1998a,b) (for electromagnetic interference or EMI shielding, for lateral guidance in automatic highways, and for television image transmission).

In relation to the structural properties, carbon fibers compete with glass, polymer, and steel fibers (Lal, 1990; Mobasher and Li, 1994, 1996; Banthia *et al*., 1994a,b, 1998; Banthia and Sheng, 1996; Pigeon *et al*., 1996; Chen and Chung, 1996c). Carbon fibers (isotropic pitch based) (Chen and Chung, 1996c; Newman, 1987) are advantageous in their superior ability to increase the tensile strength of concrete, even though the tensile strength, modulus and ductility of the isotropic pitch based carbon fibers are low compared to most other

fibers. Carbon fibers are also advantageous in the relative chemical inertness (Uomoto and Katsuki, 1994–5). PAN-based carbon fibers are also used (Ohama and Amano, 1983; Katz and Bentur, 1994; Toutanji *et al*., 1993, 1994), although they are more commonly used as continuous fibers than short fibers. Carbon-coated glass fibers (Huang *et al*., 1996, 1997) and submicron diameter carbon filaments (Shui *et al*., 1995; Xie *et al*., 1996; Fu and Chung, 1998a,b) are even less commonly used, although the former is attractive for the low cost of glass fibers and the latter is attractive for its high radio wave reflectivity (which results from the skin effect). C-shaped carbon fibers are more effective for strengthening than round carbon fibers (Kim and Park, 1998), but their relatively large diameter makes them less attractive. Carbon fibers can be used in concrete together with steel fibers, as the addition of short carbon fibers to steel fiber reinforced mortar increases the fracture toughness of the interfacial zone between steel fiber and the cement matrix (Igarashi and Kawamura, 1994). Carbon fibers can also be used in concrete together with steel bars (Bayasi and Zeng, 1997; Campione *et al*., 1999), or together with carbon fiber reinforced polymer rods (Yamada *et al*., 1995).

In relation to most functional properties, carbon fibers are exceptional compared to the other fiber types. Carbon fibers are electrically conducting, in contrast to glass and polymer fibers, which are not conducting. Steel fibers are conducting, but their typical diameter ($\geq 60\,\mu m$) is much larger than the diameter of a typical carbon fiber ($15\,\mu m$). The combination of electrical conductivity and small diameter makes carbon fibers superior to the other fiber types in the area of strain sensing and electrical conduction. However, carbon fibers are inferior to steel fibers for providing thermoelectric composites, due to the high electron concentration in steel and the low hole concentration in carbon.

Although carbon fibers are thermally conducting, addition of carbon fibers to concrete lowers the thermal conductivity (Fu and Chung, 1999), thus allowing applications related to thermal insulation. This effect of carbon fiber addition is due to the increase in air void content. The electrical conductivity of carbon fibers is higher than that of the cement matrix by about eight orders of magnitude, whereas the thermal conductivity of carbon fibers is higher than that of the cement matrix by only one or two orders of magnitude. As a result, the electrical conductivity is increased upon carbon fiber addition in spite of the increase in air void content, but the thermal conductivity is decreased upon fiber addition.

The use of pressure after casting (Delvasto *et al*., 1986), and extrusion (Shao *et al*., 1995; Park, 1998) can result in composites with superior microstructure and properties. Moreover, extrusion improves the shapability (Shao *et al*., 1995).

This chapter is focused on short carbon fiber reinforced cement–matrix composites, including concrete (with fine and coarse aggregates), mortar (with fine aggregate and no coarse aggregate) and cement paste. Previous reviews are noted (Ohama, 1989; Inagaki,

Table 10.1 Properties of isotropic-pitch-based carbon fibers

Filament diameter	$15 \pm 3\,\mu m$
Tensile strength	690 MPa
Tensile modulus	48 GPa
Elongation at break	1.4%
Electrical resistivity	$3.0 \times 10^{-3}\,\Omega\,cm$
Specific gravity	$1.6\,g\,cm^{-3}$
Carbon content	98 wt%

1991; Lin, 1994; Zheng and Feldman, 1995; Banthia, 1996; Kucharska and Brandt, 1997; Chung, 1999, 2000).

Table 10.1 shows the properties of the isotropic-pitch-based carbon fibers (15 μm in diameter, nominally 5 mm long) used by the author in the cement–matrix composites described below for the purpose of illustration.

2 Structural behavior

The properties relevant to the structural behavior of cement–matrix composites containing short carbon fibers are given in this section.

Tables 10.2 and 10.3 show the tensile strength and modulus respectively of twelve types of cement pastes (Xu and Chung, 1999a, 2000). The strength is slightly increased by the addition of methylcellulose and defoamer, but the modulus is slightly decreased by the addition of methylcellulose and defoamer. However, both strength and modulus are increased by the addition of fibers. The effectiveness of the fibers in increasing strength and modulus increases in the following order: as-received fibers, O_3-treated fibers, dichromate-treated

Table 10.2 Tensile strength (MPa) of cement pastes with and without fibers

Formulation	*As-received silica fume*	*Silane-treated silica fume*
A	1.53 ± 0.06	2.04 ± 0.06
A^+	1.66 ± 0.07	2.25 ± 0.09
A^+F	2.00 ± 0.09	2.50 ± 0.11
A^+O	2.25 ± 0.07	2.67 ± 0.09
A^+K	2.32 ± 0.08	2.85 ± 0.11
A^+S	2.47 ± 0.11	3.12 ± 0.12

Notes
A: cement + water + water reducing agent + silica fume
A^+: A + methylcellulose + defoamer.
A^+F: A^+ + as-received fibers.
A^+O: A^+ + O_3-treated fibers.
A^+K: A^+ + dichromate-treated fibers.
A^+S: A^+ + silane-treated fibers.

Table 10.3 Tensile modulus (GPa) of cement pastes with and without fibers. Refer to Note in Table 10.2

Formulation	*As-received silica fume*	*Silane-treated silica fume*
A	10.2 ± 0.7	11.5 ± 0.6
A^+	9.3 ± 0.5	10.7 ± 0.4
A^+F	10.9 ± 0.3	12.9 ± 0.7
A^+O	11.9 ± 0.3	13.1 ± 0.6
A^+K	12.7 ± 0.4	14.3 ± 0.4
A^+S	13.3 ± 0.5	15.2 ± 0.8

Table 10.4 Tensile ductility (%) of cement pastes with and without fibers. Refer to Note in Table 10.2

Formulation	*As-received silica fume*	*Silane-treated silica fume*
A	0.020 ± 0.0004	0.020 ± 0.0004
A^+	0.023 ± 0.0004	0.021 ± 0.0004
A^+F	0.025 ± 0.0003	0.024 ± 0.0004
A^+O	0.026 ± 0.0003	0.027 ± 0.0004
A^+K	0.028 ± 0.0003	0.030 ± 0.0004
A^+S	0.031 ± 0.0004	0.034 ± 0.0004

Table 10.5 Air void content (%, ± 0.12) of cement pastes with and without fibers. Refer to Note in Table 10.2

Formulation	*As-received silica fume*	*Silane-treated silica fume*
A	3.73	3.26
A^+	3.42	3.01
A^+F	5.32	4.89
A^+O	5.07	4.65
A^+K	5.01	4.49
A^+S	4.85	4.16

fibers, and silane-treated fibers. This trend applies whether the silica fume is as-received or silane-treated. For any of the formulations, silane-treated silica fume gives substantially higher strength and modulus than as-received silica fume. The highest tensile strength and modulus are exhibited by cement paste with silane-treated silica fume and silane-treated fibers. Silane treatments of silica fume and of fibers are about equally valuable in providing strengthening.

Table 10.4 shows the tensile ductility. It is slightly increased by the addition of methylcellulose and defoamer, and is further increased by the further addition of fibers. The effectiveness of the fibers in increasing the ductility also increases in the above order. This trend applies whether the silica fume is as-received or silane-treated. For any of the formulations involving surface treated fibers, silane-treated silica fume gives higher ductility than as-received silica fume. The highest ductility is exhibited by cement paste with silane-treated silica fume and silane-treated fibers.

Table 10.5 shows the air void content. It is decreased by the addition of methylcellulose and defoamer, but is increased by the further addition of fibers, whether the fibers have been surface treated or not. Among the formulations with fibers, the air void content decreases in the following order: as-received fibers, O_3-treated fibers, dichromate-treated fibers and silane-treated fibers. This trend applies whether the silica fume is as-received or silane-treated. For any of the formulations (including those without fibers), silane-treated silica fume gives lower air void content than as-received silica fume.

Tables 10.6 and 10.7 give the dynamic flexural properties of twelve types of cement pastes. Six of the types have as-received silica fume; the other six have silane-treated silica fume. The loss tangent (Table 10.6) is increased slightly by the addition of methylcellulose.

Table 10.6 Loss tangent (tan δ, ± 0.002) of cement pastes. Refer to Note in Table 10.2

Formulation	*With as-received silica fume* (Hz)			*With silane-treated silica fume* (Hz)		
	0.2	*1.0*	*2.0*	*0.2*	*1.0*	*2.0*
A	0.082	0.030	$<10^{-4}$	0.087	0.032	$<10^{-4}$
A^+	0.102	0.045	$<10^{-4}$	0.093	0.040	$<10^{-4}$
A^+F	0.089	0.033	$<10^{-4}$	0.084	0.034	$<10^{-4}$
A^+O	0.085	0.043	$<10^{-4}$	0.084	0.032	$<10^{-4}$
A^+K	0.079	0.039	$<10^{-4}$	0.086	0.035	$<10^{-4}$
A^+S	0.076	0.036	$<10^{-4}$	0.083	0.033	$<10^{-4}$

Table 10.7 Storage modulus (GPa, ± 0.03) of cement pastes. Refer to Note in Table 10.2

Formulation	*With as-received silica fume* (Hz)			*With silane-treated silica fume* (Hz)		
	0.2	*1.0*	*2.0z*	*0.2*	*1.0*	*2.0*
A	12.71	12.14	11.93	16.75	16.21	15.95
A^+	11.52	10.61	10.27	15.11	14.73	14.24
A^+F	13.26	13.75	13.83	17.44	17.92	18.23
A^+O	14.14	14.46	14.72	18.92	19.36	19.57
A^+K	15.42	16.15	16.53	19.33	19.85	20.23
A^+S	17.24	17.67	15.95	21.34	21.65	21.97

Table 10.8 Drying shrinkage strain (10^{-4}, ± 0.015) different curing ages

Formulation	*With as-received silica fume* (days)				*With silane-treated silica fume* (days)			
	1	*4*	*8*	*19*	*1*	*4*	*8*	*19*
B	1.128	3.021	3.722	4.365	1.013	2.879	3.623	4.146
BF	0.832	2.417	3.045	3.412	0.775	2.246	2.810	3.113
BO	0.825	2.355	3.022	3.373	0.764	2.235	2.793	3.014
BK	0.819	2.321	3.019	3.372	0.763	2.232	2.790	3.010
BS	0.812	2.316	2.976	3.220	0.752	2.118	2.724	2.954

Notes
B: cement + water + water reducing agent + silica fume + methylcellulose + defoamer.
BF: B + as-received fibers.
BO: B + O_3-treated fibers.
BK: B + dichromate-treated fibers.
BS: B + silane-treated fibers.

Further addition of carbon fibers decreases the loss tangent. The loss tangent decreases in the following order: as-received fibers, ozone-treated fibers, dichromate-treated fibers and silane-treated fibers, at least for the case of as-received silica fume at 0.2 Hz. The storage modulus (Table 10.7) is decreased by the addition of methylcellulose. Further addition of carbon fibers increases the storage modulus, such that the modulus increases in the

order: as-received fibers, ozone-treated fibers, dichromate-treated fibers and silane-treated fibers.

Table 10.8 gives the drying shrinkage strain of ten types of cement paste as a function of curing age. The drying shrinkage is decreased by the addition of carbon fibers, such that it decreases in the following order: as-received fibers, ozone-treated fibers, dichromate-treated fibers, and silane-treated fibers. The drying shrinkage is decreased by the use of silane-treated silica fume in place of as-received silica fume, whether fibers are present or not.

3 Thermal behavior

Table 10.9 shows the specific heat of cement pastes (Xu and Chung, 1999b, 2000). The specific heat is significantly increased by the addition of silica fume. It is further increased by the further addition of methylcellulose and defoamer. It is still further increased by the still further addition of carbon fibers. The effectiveness of the fibers in increasing the specific heat increases in the following order: as-received fibers, O_3-treated fibers, dichromate-treated fibers and silane-treated fibers. For any of the formulations, silane-treated silica fume gives higher specific heat than as-received silica fume. The highest specific heat is exhibited by the cement paste with silane-treated silica fume and silane-treated fibers. Silane treatment of fibers is more valuable than that of silica fume for increasing the specific heat.

Table 10.10 shows the thermal conductivity. It is significantly decreased by the addition of silica fume. The further addition of methylcellulose and defoamer or the still further

Table 10.9 Specific heat ($Jg^{-1}K^{-1}$, ± 0.001) of cement pastes. The value for plain cement paste (with cement and water only) is $0.736\,J\,g^{-1}K^{-1}$. Refer to Note in Table 10.2

Formulation	*As-received silica fume*	*Silane-treated silica fume*
A	0.782	0.788
A^+	0.793	0.803
A^+F	0.804	0.807
A^+O	0.809	0.813
A^+K	0.812	0.816
A^+S	0.819	0.823

Table 10.10 Thermal conductivity ($Wm^{-1}K^{-1}$, ± 0.03) of cement pastes. The value for plain cement paste (with cement and water only) is 0.53 $Wm^{-1}K^{-1}$. Refer to Note in Table 10.2

Formulation	*As-received silica fume*	*Silane-treated silica-fume*
A	0.35	0.33
A^+	0.34	0.30
A^+F	0.35	0.34
A^+O	0.38	0.36
A^+K	0.39	0.37
A^+S	0.34	0.32

addition of fibers has little effect on the density. Surface treatment of the fibers by ozone or dichromate slightly increases the thermal conductivity, whereas surface treatment of the fibers by silane has negligible effect. For any of the formulations, silane-treated silica fume gives slightly lower (or essentially the same) thermal conductivity as as-received silica fume. Silane treatments of silica fume and of fibers contribute comparably to reducing the thermal conductivity.

4 Electrical behavior

Figure 10.1 gives the volume electrical resistivity of composites at seven days of curing. The resistivity decreases much with increasing fiber volume fraction, whether a second filler (silica fume or sand) is present or not (Chen and Chung, 1995b). When sand is absent, the addition of silica fume decreases the resistivity at all fiber volume fractions except the highest volume fraction of 4.24%; the decrease is most significant at the lowest fiber volume fraction of 0.53%. When sand is present, the addition of silica fume similarly decreases the resistivity, such that the decrease is most significant at fiber volume fractions below 1%. When silica fume is absent, the addition of sand decreases the resistivity only when the fiber volume fraction is below about 0.5%; at high fiber volume fractions, the addition of sand even increases the resistivity due to the porosity induced by the sand. Thus, the addition of a second filler (silica fume or sand) that is essentially non-conducting decreases the resistivity of the composite only at low volume fractions of the carbon fibers and the maximum fiber volume fraction for the resistivity to decrease is larger when the particle size of the filler is smaller. The resistivity decrease is attributed to the improved fiber dispersion due to

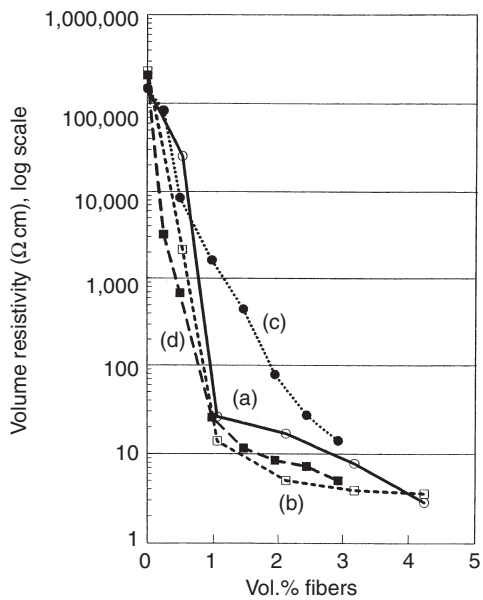

Figure 10.1 Variation of the volume electrical resistivity with carbon fiber volume fraction (Chen and Chung, 1995b). (a) Without sand, with methylcellulose, without silica fume; (b) Without sand, with methylcellulose, with silica fume; (c) With sand, with methylcellulose, without silica fume; (d) With sand, with methylcellulose, with silica fume.

the presence of the second filler. Consistent with the improved fiber dispersion is the increased flexural toughness and strength due to the presence of the second filler.

The use of both silica fume and sand results in an electrical resistivity of $3.19 \times 10^3\,\Omega\,\mathrm{cm}$ at a carbon fiber volume fraction of just 0.24 vol. %. This is an outstandingly low resistivity value compared to those of polymer-matrix composites with discontinuous conducting fillers at similar volume fractions.

Electrical conduction in cement reinforced by short carbon fibers below the percolation threshold is governed by carrier hopping across the fiber-matrix interface. The activation energy is decreased by increasing the fiber crystallinity, but is increased by using intercalated fibers. The carbon fibers contribute to hole conduction, which is further enhanced by intercalation, thereby decreasing the absolute thermoelectric power and the resistivity (Wen and Chung, 2001e).

Electric polarization induces an increase of the measured electrical resistivity of carbon fiber reinforced cement paste during resistivity measurement. The effect is diminished by increasing the conductivity of the cement paste through the use of carbon fibers that are more crystalline, the increase of the fiber content, or the use of silica fume instead of latex as an admixture. Intercalation of crystalline fibers further increases the conductivity of the composite, but it increases the extent of polarization. Voltage polarity switching effects are dominated by the polarization of the sample itself when the four-probe method is used, but are dominated by the polarization at the contact-sample interface when the two-probe method is used. Polarization reversal is faster and more complete for the latter (Wen and Chung, 2001d).

5 Radio wave reflectivity

Due to the electrical conductivity of carbon fibers, the addition of carbon fibers to cement significantly increases the ability of the composite to reflect radio waves, thus allowing EMI shielding and lateral guidance in automatic highways. However, due to the skin effect (the phenomenon in which electromagnetic radiation at a high frequency, such as 1 GHz, penetrates only the near surface region of a conductor), discontinuous carbon filaments of 0.1 μm diameter, as made from carbonaceous gases by catalytic growth, are much more effective for radio wave reflection than conventional pitch-based carbon fibers of diameter 15 μm (Fu and Chung, 1997b, 1998a,b). However, the 0.1 μm diameter filaments are less effective than the 15 μm diameter fibers as a reinforcement.

The cement–matrix composites are more effective than corresponding polymer–matrix composites for radio wave reflection, due to the slight conductivity of the cement matrix and the insulating nature of the polymer matrix. The conductivity of the cement matrix allows some electrical connectivity of the filler units, even when the filler concentration is below the percolation threshold (Fu and Chung, 1998b).

6 Cathodic protection of steel reinforcement in concrete

Cathodic protection is one of the most common and effective methods for corrosion control of steel reinforced concrete. This method involves the application of a voltage so as to force electrons to go to the steel reinforcing bar (rebar), thereby making the steel a cathode. As the steel rebar is embedded in concrete, the electrons need to go through the concrete in order to reach the rebar. However, concrete is not electrically very conductive. The use of

carbon fiber reinforced concrete for embedding the rebar to be cathodically protected facilitates cathodic protection, as the short carbon fibers enhance the conductivity of the concrete. Although the increase in conductivity is not desirable for the corrosion resistance of the embedded rebar, the presence of either silica fume or latex along with the fibers compensates for this negative effect, because the silica fume or latex reduces the water absorptivity (Hou and Chung, 2000).

For directing electrons to the steel reinforced concrete to be cathodically protected, an electrical contact is needed on the concrete. The electrical contact is electrically connected to the voltage supply. One of the choices of an electrical contact material is zinc, which is a coating deposited on the concrete by thermal spraying. It has a very low volume resistivity (thus requiring no metal mesh embedment), but it suffers from poor wear and corrosion resistance, the tendency to oxidize, high thermal expansion coefficient, and high material and processing costs. Another choice is a conductor filled polymer (Pangrazzi *et al*., 1994), which can be applied as a coating without heating, but it suffers from poor wear resistance, high thermal expansion coefficient and high material cost. Yet another choice is a metal (e.g. titanium) strip or wire embedded at one end in cement mortar, which is in the form of a coating on the steel reinforced concrete. The use of carbon fiber reinforced mortar for this coating facilitates cathodic protection, as it is advantageous to enhance the conductivity of this coating.

Due to the decrease in volume electrical resistivity associated with carbon fiber addition (0.35 vol%) to concrete (embedding steel rebar), concrete containing carbon fibers and silica fume reduces by 18% the driving voltage required for cathodic protection compared to plain concrete, and by 28% compared to concrete with silica fume. Due to the decrease in resistivity associated with carbon fiber addition (1.1 vol%) to mortar, overlay (embedding titanium wires for electrical contacts to steel reinforced concrete) in the form of mortar containing carbon fibers and latex reduces by 10% the driving voltage required for cathodic protection, compared to plain mortar overlay. In spite of the low resistivity of mortar overlay with carbon fibers, cathodic protection requires multiple metal electrical contacts embedded in the mortar at a spacing of 11 cm or less.

7 Strain sensing

Cement reinforced with short carbon fibers is capable of sensing its own strain due to the effect of strain on the volume electrical resistivity (a phenomenon known as piezoresistivity) (Chen and Chung, 1993b, 1995a, 1996a,b; Chung, 1995; Zhao *et al*., 1995; Fu and Chung, 1996, 1997a; Fu *et al*., 1996, 1997, 1998b; Mao *et al*., 1996a,b; Sun *et al*., 1998; Shi and Chung, 1999; Wen and Chung, 2000a, 2001a) and due to the effect of strain on the relative dielectric constant (a phenomenon known as direct piezoelectricity) (Wen and Chung, 2002a,b).

7.1 Piezoresistivity

Uniaxial tension of carbon fiber reinforced cement in the elastic regime causes reversible increases in the volume electrical resistivity in both longitudinal and transverse directions, such that the gage factor (fractional change in resistance per unit strain) is comparable in magnitude in the two directions (Wen and Chung, 2000a). In contrast, uniaxial compression causes reversible decreases in the resistivity in both directions (Wen and Chung, 2001a).

Table 10.11 Gage factor of carbon-fiber cement pastes under uniaxial compression and under uniaxial tension (Wen and Chung, 2000a, 2001a)

	Carbon-fiber silica-fume cement paste	*Carbon-fiber latex cement paste*
Compression		
Longitudinal	+350	+210
Transverse	−390	−80
Tension		
Longitudinal	+89	+51
Transverse	−59	−36

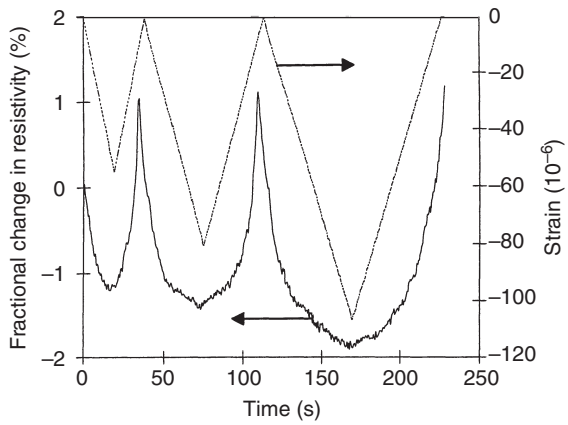

Figure 10.2 Variation of the fractional change in volume electrical resistivity with time and of the strain (negative for compressive strain) with time during dynamic compressive loading at increasing stress amplitudes within the elastic regime for carbon-fiber latex cement paste at 28 days of curing (Wen and Chung, 2001a).

Without the fibers, the resistivity changes are much smaller and less reversible. The resistivity increase is attributed to defect generation or aggravation under tension and defect healing under compression. The fractional change in resistance per unit strain (i.e. the gage factor) is higher in magnitude for carbon-fiber silica-fume cement paste than carbon-fiber latex cement paste, as shown in Table 10.11.

Figure 10.2 shows the fractional change in resistivity along the stress axis as well as the strain during repeated compressive loading at an increasing stress amplitude for carbon-fiber latex cement paste at 28 days of curing. The strain varies linearly with the stress up to the highest stress amplitude. The strain returns to zero at the end of each cycle of loading. The resistivity decreases upon loading in every cycle (due to fiber push-in) and increases upon unloading in every cycle (due to fiber pull-out). The resistivity has a net increase after the first cycle, due to very minor damage. Little further damage occurs in subsequent cycles, as shown by the resistivity after unloading not increasing much after the first cycle. The greater the strain amplitude, the more is the resistivity decrease during loading, although the

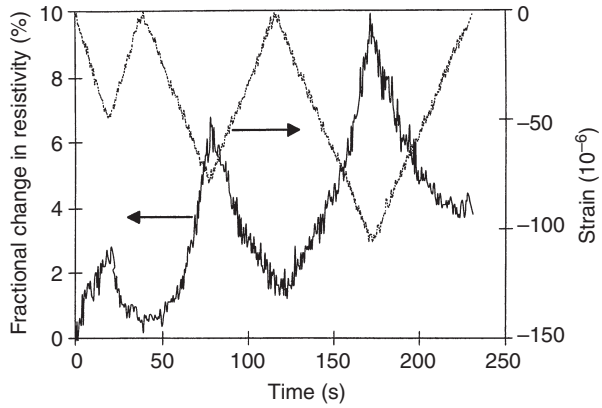

Figure 10.3 Variation of the fractional change in volume electrical resistivity with time and of the strain (negative for compressive strain) with time during dynamic compressive loading at increasing stress amplitudes within the elastic regime for carbon-fiber latex cement paste at 7 days of curing (Wen and Chung, 2001a).

resistivity and strain are not linearly related. The effects of Fig. 10.2 were similarly observed in carbon-fiber silica-fume cement paste at 28 days of curing.

Figure 10.3 gives the corresponding plots for carbon-fiber latex cement paste at 7 days of curing. Comparison of Figs 10.2 and 10.3 shows that (i) the resistivity increases upon loading at 7 days (Figs 10.3), but decreases upon loading at 28 days (Fig. 10.2); (ii) the resistivity increase upon loading at 7 days is not totally reversible, whereas the resistivity decrease upon loading at 28 days is totally reversible; and (iii) the fractional increase in resistivity upon loading is up to 10% at 7 days, but the fractional decrease in resistivity upon loading is only up to 2% at 28 days, though R_0 is similar at 7 and 28 days. The effects in Fig. 10.3 were similarly observed in carbon-fiber silica-fume cement paste at 7 days. The changeover from the 7-day behavior to the 28-day behavior occurs between 7 and 14 days.

Although the fractional change in resistivity upon loading is larger at 7 days (Fig. 10.3) than at 28 days (Fig. 10.2) for carbon-fiber latex cement paste, the greater reversibility upon unloading and the less noise in the resistivity variation at 28 days makes the behavior at 28 days more attractive than that at 7 days for use in resistance-based strain sensing. In practice, concrete is used in a fully cured state (exceeding 28 days of curing). Therefore, the behavior at 28 days is practically more important than that at 7 days. Nevertheless, the behavior at 7 days is of fundamental interest.

Comparison of Figs 10.4 and 10.3 (both at 7 days) shows that the effects are qualitatively similar with fibers (Fig. 10.3) and without fibers (Fig. 10.4), though (i) the fractional change in resistivity is larger in the presence of fibers; and (ii) the resistivity increase upon loading is more reversible in the presence of fibers. Thus, the origins of the effects in Figs 10.4 and 10.3 are basically similar, though the presence of fibers, which are electrically conductive, in Fig. 10.3 adds to the types of defects that are generated upon loading and the fiber-related defects make the resistivity changes more pronounced and more reversible.

Comparison of Figs 10.5 and 10.2 (both at 28 days) shows that the effects are qualitatively and quantitatively different between latex cement paste (Fig. 10.5) and carbon-fiber latex

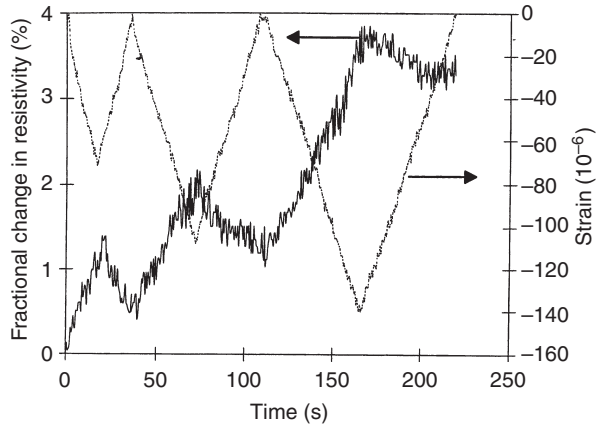

Figure 10.4 Variation of the fractional change in volume electrical resistivity with time and of the strain (negative for compressive strain) with time during dynamic compressive loading at increasing stress amplitudes within the elastic regime for latex cement paste at 7 days of curing (Wen and Chung, 2001a).

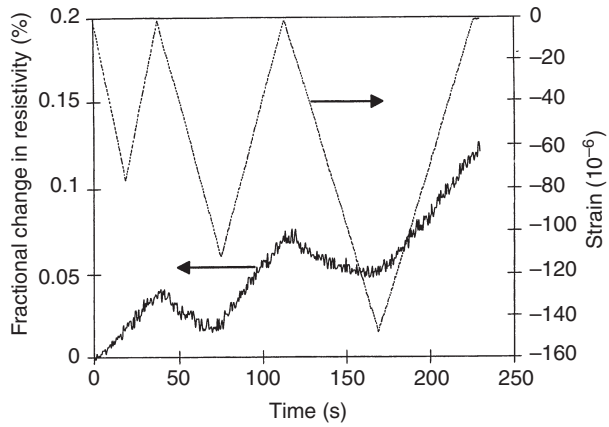

Figure 10.5 Variation of the fractional change in volume electrical resistivity with time and of the strain (negative for compressive strain) with time during dynamic compressive loading at increasing stress amplitudes within the elastic regime for latex cement paste at 28 days of curing (Wen and Chung, 2001a).

cement paste (Fig. 10.2). In the presence of carbon fibers, the resistivity decreases reversibly upon loading; in the absence of fibers, the resistivity mainly increases upon unloading.

Figures 10.2–10.5 show that the effect of carbon fibers on the variation of the resistivity with strain is more drastic at 28 days than at 7 days.

7.2 Direct piezoelectricity

The direct piezoelectric effect was observed in cement pastes by voltage measurement (Sun *et al*., 2000) and by measurement of the relative dielectric constant (10 kHz) (Wen and

Chung, 2001b) in the stress direction during repeated compressive loading (Wen and Chung, 2002a,b). The effect is particularly large when the cement paste contains short steel fibers (8 μm diameter, 0.18 vol. %) and polyvinyl alcohol (0.16 vol. %). In this case, the longitudinal piezoelectric coupling coefficient is $2.5 \times 10^{-11}\,\mathrm{mV}^{-1}$ and the piezoelectric voltage coefficient is $1.1 \times 10^{-3}\,\mathrm{m}^2\,\mathrm{C}^{-1}$ (10 kHz) (Wen and Chung, 2002a).

8 Damage sensing

Figure 10.6 (Bontea *et al*., 2000) shows the fractional change in longitudinal resistance, strain and stress during repeated compressive loading at increasing and decreasing stress amplitudes for carbon fiber concrete at 28 days of curing. The highest stress amplitude is 60% of the compressive strength. A group of cycles in which the stress amplitude increases cycle by cycle and then decreases cycle by cycle back to the initial low stress amplitude is hereby referred to as a group. Figure 10.6 shows the results for three groups. The strain returns to zero at the end of each cycle for any of the stress amplitudes, indicating elastic behavior. The resistance decreases upon loading in each cycle, as in Fig. 10.2. An extra peak at the maximum stress of a cycle grows as the stress amplitude increases, resulting in two peaks per cycle. The original peak (strain induced) occurs at zero stress, while the extra peak (damage induced) occurs at the maximum stress. Hence, during loading from zero stress within a cycle, the resistance drops and then increases sharply, reaching the maximum resistance of the extra peak at the maximum stress of the cycle. Upon subsequent unloading, the resistance decreases and then increases as unloading continues, reaching the maximum resistance of the original peak at zero stress. In the part of this group where the stress

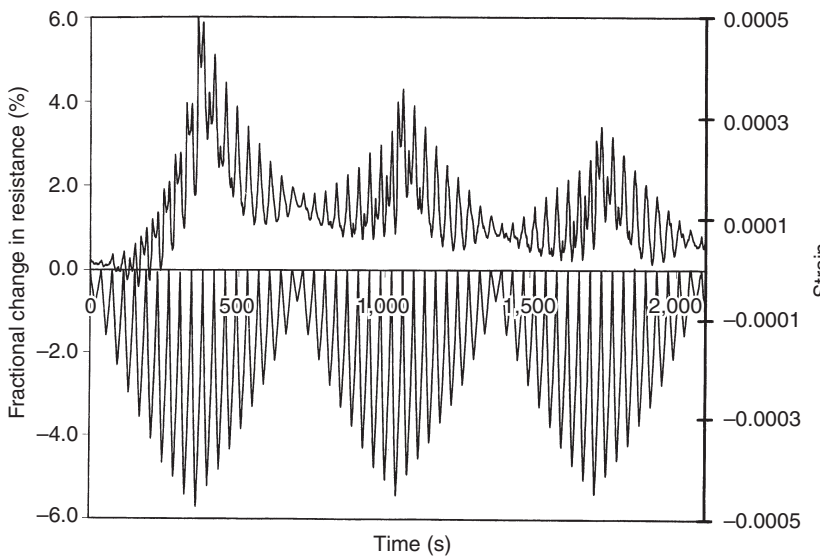

Figure 10.6 Fractional change in resistance and strain during repeated compressive loading at increasing and decreasing stress amplitudes, the highest of which was 60% of the compressive strength, for carbon fiber concrete at 28 days of curing (Bontea *et al*., 2000).

amplitude decreases cycle by cycle, the extra peak diminishes and disappears, leaving the original peak as the sole peak. In the part of the second group where the stress amplitude increases cycle by cycle, the original peak (peak at zero stress) is the sole peak, except that the extra peak (peak at the maximum stress) returns in a minor way (more minor than in the first group) as the stress amplitude increases. The extra peak grows as the stress amplitude increases, but, in the part of the second group in which the stress amplitude decreases cycle by cycle, it quickly diminishes and vanishes, as in the first group. Within each group, the amplitude of resistance variation increases as the stress amplitude increases and decreases as the stress amplitude subsequently decreases.

The greater the stress amplitude, the larger and the less reversible is the damage-induced resistance increase (the extra peak). If the stress amplitude has been experienced before, the damage-induced resistance increase (the extra peak) is small, as shown by comparing the result of the second group with that of the first group (Fig. 10.6), unless the extent of damage is large (Fig. 10.7 for a highest stress amplitude of $>90\%$ the compressive strength). When the damage is extensive (as shown by a modulus decrease), damage-induced resistance increase occurs in every cycle, even at a decreasing stress amplitude, and it can overshadow the strain-induced resistance decrease (Fig. 10.7). Hence, the damage-induced resistance increase occurs mainly during loading (even within the elastic regime), particularly at a stress above that in prior cycles, unless the stress amplitude is high and/or damage is extensive.

At a high stress amplitude, the damage-induced resistance increase cycle by cycle as the stress amplitude increases causes the baseline resistance to increase irreversibly (Fig. 10.7). The baseline resistance in the regime of major damage (with a decrease in modulus)

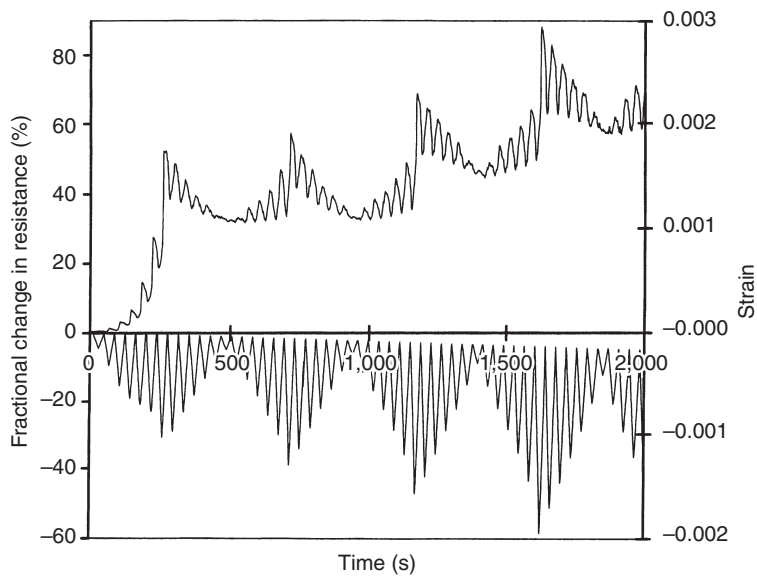

Figure 10.7 Fractional change in resistance and strain during repeated compressive loading at increasing and decreasing stress amplitudes, the highest of which was $>90\%$ of the compressive strength, for carbon fiber concrete at 28 days of curing (Bontea *et al*., 2000).

provides a measure of the extent of damage (i.e. condition monitoring). This measure works in the loaded or unloaded state. In contrast, the measure using the damage-induced resistance increase (Fig. 10.6) works only during stress increase and indicates the occurrence of damage (whether minor or major) as well as the extent of damage.

The damage causing the partially reversible damage-induced resistance increase is probably mainly associated with partially reversible degradation of the fiber-matrix interface. The reversibility rules out fiber fracture as the main type of damage, especially at a low stress amplitude. At a high stress amplitude, the extent of reversibility diminishes and fiber fracture may contribute to causing the damage. Fiber fracture can occur during the opening of a crack that is bridged by a fiber. The fiber-matrix interface degradation may be associated with slight fiber pull-out upon slight crack opening for cracks that are bridged by fibers. The severity of the damage-induced resistance increase supports the involvement of the fibers in the damage mechanism.

9 Temperature sensing through the thermistor effect

A thermistor is a thermometric device consisting of a material (typically a simiconductor, but in this case a cement paste) whose electrical resistivity decreases with rise in temperature.

Figure 10.8 (Wen and Chung, 1999b) shows the current–voltage characteristic of carbon-fiber (0.5% by weight of cement) silica-fume (15% by weight of cement) cement paste at 38 °C during stepped heating. The characteristic is linear below 5 V and deviates positively from linearity beyond 5 V. The resistivity is obtained from the slope of the linear portion. The voltage at which the characteristic starts to deviate from linearity is referred to as the critical voltage.

Figure 10.9 shows a plot of the resistivity versus temperature during heating and cooling for carbon-fiber silica-fume cement paste. The resistivity decreases upon heating and the effect is quite reversible upon cooling. That the resistivity is slightly increased after a heating-cooling cycle is probably due to thermal degradation of the material. From the Arrhenius plot of log conductivity (conductivity = 1/resistivity) versus reciprocal absolute temperature, the activation energy was found to be 0.390 ± 0.014 and 0.412 ± 0.017 eV during heating and cooling, respectively.

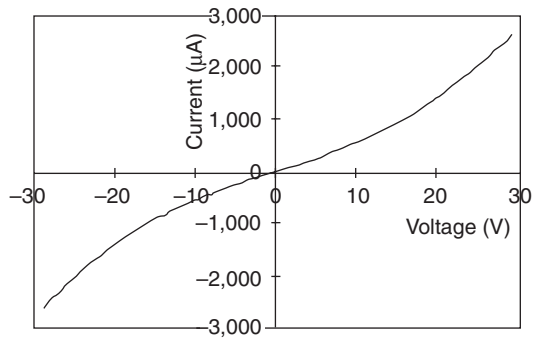

Figure 10.8 Current–voltage characteristic of carbon-fiber silica-fume cement paste at 38 °C during stepped heating (Wen and Chung, 1999b).

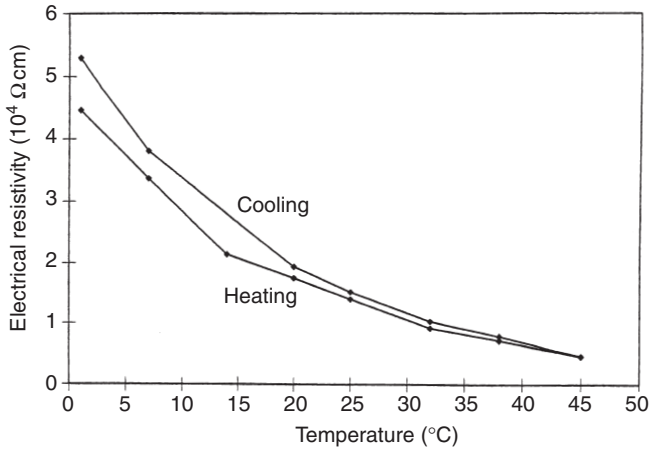

Figure 10.9 Plot of volume electrical resistivity versus temperature during heating and cooling for carbon-fiber silica-fume cement paste (Wen and Chung, 1999b).

Table 10.12 Resistivity, critical voltage and activation energy of five types of cement paste (Wen and Chung, 1999b)

Formulation	*Resistivity at 20°C* (Ω cm)	*Critical voltage at 20°C* (V)	*Activation energy* (eV)	
			Heating	*Cooling*
Plain	$(4.87 \pm 0.37) \times 10^5$	10.80 ± 0.45	0.040 ± 0.006	0.122 ± 0.006
Silica fume	$(6.12 \pm 0.15) \times 10^5$	11.60 ± 0.37	0.035 ± 0.003	0.084 ± 0.004
Carbon fibers + silica fume	$(1.73 \pm 0.08) \times 10^4$	8.15 ± 0.34	0.390 ± 0.014	0.412 ± 0.017
Latex	$(6.99 \pm 0.12) \times 10^5$	11.80 ± 0.31	0.017 ± 0.001	0.025 ± 0.002
Carbon fibers + latex	$(9.64 \pm 0.08) \times 10^4$	8.76 ± 0.35	0.018 ± 0.001	0.027 ± 0.002

Results similar to those of carbon-fiber silica-fume cement paste were obtained with carbon-fiber (0.5% by weight of cement) latex (20% by weight of cement) cement paste, silica-fume cement paste, latex cement paste, and plain cement paste. However, for all these four types of cement paste, (i) the resistivity is higher by about an order of magnitude; and (ii) the activation energy is lower by about an order of magnitude, as shown in Table 10.12. The critical voltage is higher when fibers are absent (Table 10.12).

10 Thermoelectric behavior

The Seebeck effect is a thermoelectric effect which is the basis for thermocouples for temperature measurement. This effect involves charge carriers moving from a hot point to a cold point within a material, thereby resulting in a voltage difference between the two points. The Seebeck coefficient is the voltage difference (hot minus cold) per unit temperature difference (hot minus cold) between the two points. Negative carriers (electrons) make it more negative and positive carriers (holes) make it more positive.

Eight types of cement paste were studied comparitively, namely (i) plain cement paste (consisting of just cement and water); (ii) silica-fume cement paste (consisting of cement, water, and silica fume); (iii) carbon-fiber silica-fume cement paste (consisting of cement, water, silica fume, methylcellulose, defoamer, and carbon fibers in the amount of 0.5% by weight of cement); (iv) carbon-fiber silica-fume cement paste (same as (iii) except for having carbon fibers in the amount of 1.0% by weight of cement); (v) carbon-fiber silica-fume cement paste (same as (iii) except for having carbon fibers in the amount of 1.5% by weight of cement); (vi) latex cement paste (consisting of cement, water, latex, and antifoam); (vii) carbon-fiber latex cement paste (consisting of cement, water, latex, antifoam, and carbon fibers in the amount of 0.5% by weight of cement; and (viii) carbon-fiber latex cement paste (same as (vii) except for having carbon fibers in the amount of 1.0% by weight of cement).

Table 10.13 (Wen and Chung, 1999c, 2000b–d) shows the Seebeck coefficient (with copper as the reference) and the absolute thermoelectric power. A positive value of the absolute thermoelectric power indicates p-type (hole) behavior; a negative value indicates n-type (electron) behavior. All types of cement paste studied are n-type except pastes (iv) and (v), which were p-type. The higher the fiber content, the less n-type (the more p-type) is the paste, whether silica fume or latex is present. Without fibers, the absolute thermoelectric power is $-2\ \mu V/°C$, whether silica fume and latex are present or not. This is consistent with the similar values of the electrical conductivity for cement pastes with silica fume and with latex, but without fibers. Thus, silica fume or latex addition does not have much influence on the thermoelectric power when fibers are absent, but carbon fiber addition does by enhancing the hole conduction.

As shown in Table 10.13, the thermopower results obtained during heating and cooling are very close. Figure 10.10 shows the variation of the Seebeck voltage versus the temperature difference during heating and cooling for paste (iii). With fibers present, the variation is linear and essentially identical during heating and cooling. Without fibers, the variation is non-linear and hysteretic (i.e. not totally reversible upon cooling subsequent to heating). Thus, although the fiber addition does not increase the magnitude of the absolute

Table 10.13 Seebeck coefficient (μV/°C) and absolute thermoelectric power (μV/°C) of eight types of cement paste (Wen and Chung, 1999c, 2000b,c,d)

Cement paste	*Heating*		*Cooling*	
	*Seebeck coefficient**	*Absolute thermoelectric power*	*Seebeck coefficient**	*Absolute thermoelectric power*
(i) Plain	0.35 ± 0.03	−1.99 ± 0.03	0.38 ± 0.05	−1.96 ± 0.05
(ii) Silica fume	0.31 ± 0.02	−2.03 ± 0.02	0.36 ± 0.03	−1.98 ± 0.03
(iii) 0.5% fibers + silica fume	1.45 ± 0.09	−0.89 ± 0.09	1.45 ± 0.09	−0.89 ± 0.09
(iv) 1.0% fibers + silica fume	2.82 ± 0.11	+0.48 ± 0.11	2.82 ± 0.11	+0.48 ± 0.11
(v) 1.5% fibers + silica fume	3.10 ± 0.14	+0.76 ± 0.14	3.10 ± 0.14	+0.76 ± 0.14
(vi) Latex	0.28 ± 0.02	−2.06 ± 0.02	0.30 ± 0.02	−2.04 ± 0.02
(vii) 0.5% fibers + latex	1.20 ± 0.05	−1.14 ± 0.05	1.20 ± 0.05	−1.14 ± 0.05
(viii) 1.0% fibers + latex	2.10 ± 0.08	−0.24 ± 0.08	2.10 ± 0.08	−0.24 ± 0.08

Note
* With copper as the reference.

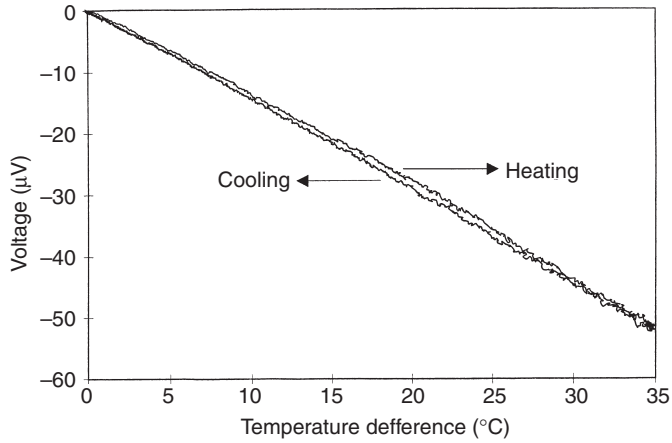

Figure 10.10 Variation of the Seebeck voltage (with copper as the reference) versus the temperature difference during heating and cooling for carbon-fiber silica-fume cement paste (Wen and Chung, 1999c).

thermoelectric power, it enhances the linearity and reversibility of the Seebeck effect. This enhancement is attributed to the increase in the contribution of holes to the electrical conduction and the association of hole conduction to conduction through the fibers.

The absolute thermoelectric power monotonically becomes less negative (more positive) as the fiber content increases through the percolation threshold, which is at a fiber content between 0.5% and 1.0% by weight of cement. The change of the absolute thermoelectric power from negative to positive values occurs at a fiber content between 0.5% and 1.0% by weight of cement when silica fume is present. This means that at this fiber content, which happens to be the percolation threshold, compensation takes place between the electron contribution from the cement matrix and the hole contribution from the fibers. It should be noted that, at any fiber content, electrons and holes contribute additively to the electrical conductivity, but subtractively to the thermopower. The correlation between the percolation threshold and change in sign of the absolute thermoelectric power is reasonable since the fibers dominate the conduction by means of holes above the percolation threshold and the cement matrix dominates the conduction by means of electrons below the percolation threshold. In the presence of latex instead of silica fume, the highest fiber content investigated was 1.0% by weight of cement and a change in sign of the absolute thermoelectric power was not observed, even though the percolation threshold is also between fiber contents of 0.5% and 1.0% by weight of cement for the case of latex. Although a change in sign of the absolute thermoelectric power was not observed for the case of latex, the absolute thermoelectric power is a negative value of a very small magnitude at a fiber content of 1.0% by weight of cement and the magnitude of the absolute thermoelectric power decreases monotonically with increasing fiber content. Based on this trend, it is highly probable that a change in sign would occur just above 1.0% by weight of cement for the case of latex. That a change in sign of the absolute thermoelectric power does not occur at the percolation threshold (but probably just above the threshold) is attributed to the low conductivity of carbon-fiber latex cement paste compared to carbon-fiber silica-fume cement paste at the same fiber content

and the associated weaker hole conduction in the latex case. This is consistent with the observation that, at the same fiber content (whether 0.5% or 1.0% by weight of cement), the absolute thermoelectric power is more positive for the latex case than the silica fume case (Table 10.13).

The use of steel fibers instead of carbon fibers results in highly negative (as negative $-68\,\mu V/°C$) values of the absolute thermoelectric power, as steel fibers involve electron conduction whereas carbon fibers involve hole conduction (Wen and Chung, 2000a–d). The highly negative values mean that the use of steel fibers gives a superior thermoelectric material then the use of carbon fibers.

A cement-based thermocouple in the form of a junction between dissimilar cement pastes exhibits thermocouple sensitivity $70 \pm 7\,\mu V/°C$ (Wen and Chung, 2001g). The dissimilar cement pastes are steel fiber cement paste (n-type) and carbon-fiber silica-fume cement paste (p-type). The junction is made by pouring the cement pastes side by side. In addition to serving as a thermocouple junction, the junction provides electric current rectification (Wen and Chung, 2001f).

11 Corrosion resistance

Carbon fibers decrease the corrosion resistance of steel rebar in concrete, mainly due to the decrease in the volume electrical resistivity of concrete. However, the negative effect can be compensated by adding either silica fume or latex. Silica fume is more effective than latex for improving the corrosion resistance of carbon fiber concrete. This is mainly because silica fume reduces the water absorptivity. The small increases in electrical resistivity of carbon fiber concrete after adding either silica fume or latex contribute only slightly to the effect on corrosion. Corrosion of rebar in concrete with silica fume and carbon fibers is inactive in $Ca(OH)_2$ solution, but active in NaCl solution. However, the corrosion resistance in NaCl is better than rebar in plain concrete and similar to that of rebar in latex concrete without fibers (Hou and Chung, 2000).

12 Conclusion

Short carbon fiber cement–matrix composites exhibit attractive tensile and flexural properties, low drying shrinkage, high specific heat, low thermal conductivity, high electrical conductivity, high corrosion resistance, and weak thermoelectric behavior. Moreover, they facilitate the cathodic protection of steel reinforcement in concrete, and have the ability to sense their own strain, damage, and temperature. The strain sensing is associated with piezoresistivity and piezoelectricity.

Acknowledgment

This work was supported in part by the National Science Foundation of USA.

References

Akihama, S., Suenaga, T., and Banno, T. (1984). *Int. J. Cem. Composites & Lightweight Concrete*, **6** (3), 159.

Ali, A. and Ambalavanan, R. (1998). *Indian Concrete J.*, **72** (12), 669.

Banthia, N. (1996). *Indian Concrete J.*, **70** (10), 533.

Banthia, N., Djeridane, S., and Pigeon, M. (1992). *Cem. Concr. Res.*, **22** (5), 804.
Banthia, N., Moncef, A., Chokri, K., and Sheng, J. (1994a). *Can. J. Civil Eng.*, **21** (6), 999.
Banthia, N., Chokri, K., Ohama, Y., and Mindess, S. (1994b). *Adv. Cem. Based Mater.*, **1** (3), 131.
Banthia, N. and Sheng, J. (1996). *Cem. Concr. Composites*, **18** (4), 251.
Banthia, N., Yan, C., and Sakai, K. (1998). *Com. Concr. Composites*, **20** (5), 393.
Bayasi, M. Z. and Zeng, J. (1997). *ACI Structural J.*, **94** (4), 442.
Bontea, D., Chung, D. D. L., and Lee, G. C. (2000). *Cem. Concr. Res.*, **30** (4), 651.
Brandt, A. M. and Kucharska, L. (1996). *Materials for the New Millennium*, Proc. Mater. Eng. Conf., Vol. 1, ASCE, New York, 271–280.
Brousseau, R. J. and Pye, G. B. (1997). *ACI Mater. J.*, **94** (4), 306.
Campione, G., Mindess, S., and Zingone, G. (1999). *ACI Mater. J.*, **96** (1), 27.
Chen, P. and Chung, D. D. L. (1993a). *Composites*, **24** (1), 33.
Chen, P. and Chung, D. D. L. (1993b). *Smart Mater. Struct.*, **2**, 22.
Chen, P. and Chung, D. D. L. (1993c). *Smart Mater. Struct.*, **2**, 181.
Chen, P. and Chung, D. D. L. (1995a). *J. Am. Ceram. Soc.*, **78** (3), 816.
Chen, P. and Chung, D. D. L. (1995b). *J. Electron. Mater.*, **24** (1), 47.
Chen, P. and Chung, D. D. L. (1996a). *Composites*, Part B, **27B**, 11.
Chen, P. and Chung, D. D. L. (1996b). *ACI Mater. J.*, **93** (4), 341.
Chen, P. and Chung, D. D. L. (1996c). *ACI Mater. J.*, **93** (2), 129.
Chen, P. Fu, X., and Chung, D. D. L. (1995). *Cem. Concr. Res.*, **25** (3), 491.
Chen, P. Fu, X., and Chung, D. D. L. (1997). *ACI Mater. J.*, **94** (2), 147.
Chung, D. D. L. (1995). *Smart Mater. Struct.*, **4**, 59.
Chung, D. D. L. (1999). *TANSO* (190), 300.
Chung, D. D. L. (2000). *Smart Mater. Struct.*, **9** (4), 389.
Clemena, G. G. (1988). *Materials Performance*, **27** (3), 19.
Delvasto, S., Naaman, A. E., and Throne, J. L. (1986). *Int. J. Cem. Composites & Lightweight Concrete*, **8** (3), 181.
Fu, X. and Chung, D. D. L. (1995). *Cem. Concr. Res.*, **25** (4), 689.
Fu, X. and Chung, D. D. L. (1996). *Cem. Concr. Res.*, **26** (1), 15.
Fu, X. and Chung, D. D. L. (1996). *Cem. Concr. Res.*, **26** (10), 1467.
Fu, X. and Chung, D. D. L. (1997a). *Cem. Concr. Res.*, **27** (9), 1313.
Fu, X. and Chung, D. D. L. (1997b). *Cem. Concr. Res.*, **27** (2), 314.
Fu, X. and Chung, D. D. L. (1998a). *Cem. Concr. Res.*, **28** (6), 795.
Fu, X. and Chung, D. D. L. (1998b). *Carbon*, **36** (4), 459.
Fu, X. and Chung, D. D. L. (1999). *ACI Mater. J.*, **96** (4), 455.
Fu, X. Lu, W., and Chung, D. D. L. (1996). *Cem. Concr. Res.*, **26** (7), 1007.
Fu, X. Ma, E., Chung, D. D. L., and Anderson, W. A. (1997). *Cem. Concr. Res.*, **27** (6), 845.
Fu, X. Lu, W. and Chung, D. D. L. (1998a). *Carbon*, **36** (9), 1337.
Fu, X. Lu, W. and Chung, D. D. L. (1998b). *Cem. Concr. Res.*, **28** (2), 183.
Fujiwara, T. and Ujie, H. (1987). *Tohoku Kogyo Daigaku Kiyo, 1: Rikogakuhen* (7), 179.
Furukawa, S., Tsuji, Y., and Otani, S. (1987). *Proc. 30th Japan Congress on Materials Research*, Soc. Mater. Sci., Kyoto, Japan, 149–152.
Huang, C. M., Zhu, D., Dong, C. X., Kriven, W. M., Loh, R., and Huang, J. (1996). *Ceramic Eng. Sci. Proc.*, **17** (4), 258.
Huang, C. M., Zhu, D., Cong, X., Kriven, W. M., Loh, R. R., and Huang, J. (1997). *J. Am. Ceramic Soc.*, **80** (9), 2326.
Hou, J. and Chung, D. D. L. (1997). *Cem. Concr. Res.*, **27** (5), 649.
Hou, J. and Chung, D. D. L. (2000). *Corrosion Sci.*, **42** (9), 1489.
Igarashi, S., and Kawamura, M. (1994). *Doboku Gakkai Rombun-Hokokushu/Proc. Japan Soc. Civil Eng.*, (502), pt 5–25, 83.
Inagaki, M. (1991). *Carbon*, **29** (3), 287.

Kamakura, M., Shirakawa, K., Nakagawa, K., Ohta, K., and Kashihara, S. (1983). *Sumitomo Metals*.
Katz, A. and Bentur, A. (1994). *Cem. Concr. Res.*, **24** (2), 214.
Katz, A., Li, V. C., and Kazmer, A. (1995). *J. Materials Civil Eng.*, **7** (2), 125.
Kim, T.-J., and Park, C.-K. (1998). *Cem. Concr. Res.*, **28** (7), 955.
Kucharska, L. and Brandt, A. M. (1997). *Archives of Civil Engineering*, **43** (2), 165.
Lal, A. K. (1990), *Batiment Int./Building Research & Practice*, **18** (3), 153.
Larson, B. K., Drzal, L. T., and Sorousian, P. (1990). *Composites*, **21** (3), 205.
Lee, J., and Batson, G. (1996). *Materials for the New Millennium*, Proc. 4th Mater. Eng. Conf., Vol. 2, ASCE, New York, 887–896.
Lin, S.-S. (1994). *SAMPE J.*, **30** (5), 39.
Mao, Q., Zhao, B., Shen, D., and Li, Z. (1996a). *J. Wuhan U. Tech.*, Mater. Sci. Ed., **11** (3), 41.
Mao, Q., Zhao, B., Shen, D., and Li, Z. (1996b). *Fuhe Cailiao Xuebao/Acta Materiae Compositae Sinica*, **13** (4), 8.
Mobasher, B. and Li, C. Y. (1994). *Infrastructure: New Materials and Methods of Repair*, Proc. Mater. Eng. Conf. (804), ASCE, New York, 551–558.
Mobasher, B. and Li, C. Y. (1996). *ACI Mater. J.*, **93** (3), 284.
Newman, J. W. (1987). *Int. SAMPE Symp. Exhib.*, **32**, SAMPE, Covina, CA, 938–944.
Ohama, Y. and Amano, M. (1983). *Proc. 27th Japan Congress on Materials Research*, Soc. Mater. Sci., Kyoto, Japan, 187–191.
Ohama, Y., Amano, M., and Endo, M. (1985). *Concrete Int.: Design & Construction*, **7** (3), 58.
Ohama, Y. (1989). *Carbon*, **27** (5), 729.
Pangrazzi, R., Hartt, W. H., and Kessler, R. (1994). *Corrosion* (Houston), **50** (3), 186.
Park, C. (1998). Nippon Seramikkusu Kyokai *Gakujutsu Ronbunshi – J. Ceramic Soc. Japan*, **106** (1231), 268.
Park, S. B. and Lee, B. I. (1990). *High Temperatures – High Pressures*, **22** (6), 663.
Park, S. B. and Lee, B. I. (1993). *Cem. Concr*. *Composites*, **15** (3), 153.
Park, S. B, Lee, B. I., and Lim, Y. S. (1991). *Cem. Concr. Res.*, **21** (4), 589.
Pigeon, M., Azzabi, M., and Pleau, R. (1996). *Cem. Concr. Res.*, **26** (8), 1163.
Saito, K., Kawamura, N., and Kogo, Y. (1989). *Advanced Materials: The Big Payoff*, National SAMPE Technical Conf., **21**, Covina, CA, 796–802.
Shao, Y., Marikunte, S., and Shah, S. P. (1995). *Concrete Int.*, **17** (4), 48.
Shui, Z., Li, J., Huang, F., and Yang, D. (1995). *J. Wuhan Univ. Tech.*, Mater. Sci. Ed., **10** (4), 37.
Shi, Z. and Chung, D. D. L. (1999). *Cem. Concr. Res.*, **29** (3), 435.
Shimizu, Y., Nishikata, A., Maruyama, N., and Sugiyama, A. (1986). *Terebijon Gakkaishi/J. Inst. Television Engineers of Japan*, **40** (8), 780.
Shinozaki, Y. (1990). *Adv. Mater.: Looking Ahead to the 21st Century*, Proc. 22nd National SAMPE Technical, Conf. **22**, SAMPE, Covina, CA, 986–997.
Soroushian, P. (1990). *Construction Specifier*, **43** (12), 102.
Soroushian, P., Aouadi, F., and Nagi, M. (1991). *ACI Mater. J.*, **88** (1), 11.
Soroushian, P., Nagi, M., and Hsu, J. (1992a). *ACI Mater. J.*, **89** (3), 267.
Soroushian, P., Nagi, M., and Okwuegbu, A. (1992b). *ACI Mater. J.*, **89** (5), 491.
Sugama, T., Kukacka, L. E., Carciello, N., and Galen, B. (1988). *Cem. Concr. Res.*, **18** (2), 290.
Sugama, T., Kukacka, L. E., Carciello, N., and Stathopoulos, D. (1989). *Cem. Concr. Res.*, **19** (3), 355.
Sun, M., Li, Z., Mao, Q., and Shen, D. (1998a). *Cem. Concr. Res*., **28** (4), 549.
Sun, M., Li, Z., Mao, Q., and Shen, D. (1998b). *Cem. Concr. Res*., **28** (12), 1707.
Sun, M., Mao, Q., and Li, Z. (1998). *J. Wuhan U. Tech.*, Mater. Sci. Ed., **13** (4), 58.
Sun, M., Liu, Q., Li, Z., and Hu, Y. (2000). *Cem. Concr. Res.,* **30** (10), 1593.
Toutanji, H. A., El-Korchi, T., Katz, R. N., and Leatherman, G. L. (1993). *Cem. Concr. Res.*, **23** (3), 618.
Toutanji, H. A., El-Korchi, T., and Katz, R. N. (1994). *Com. Con. Composites*, **16** (1), 15.

Uomoto, T. and Katsuki, F. (1994–5). *Doboku Gakkai Rombun-Hokokushu/Proc. Japan Soc. Civil Engineers* (490), pt 5–23, 167.
Urano, T., Murakami, K., Mitsui, Y., and Sakai, H. (1996). *Composites – Part A: Applied Science & Manufacturing*, **27** (3), 183.
Wang, X., Wang, Y., and Jin, Z. (1998). *Fuhe Cailiao Xuebao/Acta Materiae Compositae Sinica*, **15** (3), 75.
Wen, S. and Chung, D. D. L. (1999a). *Cem. Concr. Res.*, **29** (3), 445.
Wen, S. and Chung, D. D. L. (1999b). *Cem. Concr. Res.*, **29** (6), 961.
Wen, S. and Chung, D. D. L. (1999c). *Cem. Concr. Res.*, **29** (12), 1989.
Wen, S. and Chung, D. D. L. (2000a). *Cem. Concr. Res.*, **30** (8), 1289.
Wen, S. and Chung, D. D. L. (2000b). *Cem. Concr. Res.*, **30** (4), 661.
Wen, S. and Chung, D. D. L. (2000c). *Cem. Concr. Res.*, **30** (8), 1295.
Wen, S. and Chung, D. D. L. (2000d). *J. Mater. Res.,* **15** (12), 2844.
Wen, S. and Chung, D. D. L. (2001a). *Cem. Concr. Res.,* **31** (2), 297.
Wen, S. and Chung, D. D. L. (2001b). *Cem. Concr. Res.,* **31** (4), 665.
Wen, S. and Chung, D. D. L. (2001c). *J. Electron. Mater.,* **30** (11), 1448.
Wen, S. and Chung, D. D. L. (2001d). *Cem. Concr. Res.,* **31** (2), 141.
Wen, S. and Chung, D. D. L. (2001e). *Carbon*, **39**, 369.
Wen, S. and Chung, D. D. L. (2001f). *Cem. Concr. Res.,* **31** (2), 129.
Wen, S. and Chung, D. D. L. (2001g). *Cem. Concr. Res.,* **31** (3), 507.
Wen, S. and Chung, D. D. L. (2001h). *Cem. Concr. Res*., **31** (4), 673.
Wen, S. and Chung, D. D. L. (2002a). *Cem. Concr. Res*., **32** (3), 335.
Wen, S. and Chung, D. D. L. (2002b). *Cem. Concr. Res*., **32** (9), 1429.
Xie, P., Gu, P., and Beaudoin, J. J. (1996). *J. Mater. Sci.*, **31** (15), 4093.
Xu, Y. and Chung, D. D. L. (1999a). *Cem. Concr. Res.*, **29** (5), 773.
Xu, Y. and Chung, D. D. L. (1999b). *Cem. Concr. Res.*, **29** (7), 1117.
Xu, Y. and Chung, D. D. L. (2000). *ACI Mater. J.*, **97** (3), 333.
Yamada, T., Yamada, K., Hayashi, R., and Herai, T. (1991). *Int. SAMPE Symp. Exhib.*, **36**, SAMPE, Covina, CA, pt 1, 362–371.
Yamada, T., Yamada, K., and Kubomura, K. (1995). *J. Composite Mater.*, **29** (2), 179.
Zayat, K. and Bayasi, Z. (1996). *ACI Mater. J.*, **93** (2), 178.
Zhao, B., Li, Z., and Wu, D. (1995). *J. Wuhan Univ. Tech.*, Mater. Sci. Ed., **10** (4), 52.
Zheng, Z. and Feldman, D. (1995). *Progress in Polymer Science*, **20** (2), 185.
Zhu, M. and Chung, D. D. L. (1997). *Cem. Concr. Res.*, **27** (12), 1829.
Zhu, M., Wetherhold, R. C., and Chung, D. D. L. (1997). *Cem. Concr. Res.*, **27** (3), 437.